Heteropolynuclear Metamagnet Showing Spin Canting and Single-Crystal to Single-Crystal Phase Transformation

ARTICLE *in* CHEMISTRY OF MATERIALS · MARCH 2007

Impact Factor: 8.35 · DOI: 10.1021/cm062801s

4 AUTHORS, INCLUDING:

Ji Zheng
Chinese Academy of Sciences
128 PUBLICATIONS **2,629** CITATIONS

SEE PROFILE

Stuart R. Batten
Monash University (Australia)
311 PUBLICATIONS **14,180** CITATIONS

SEE PROFILE

Heteropolynuclear Metamagnet Showing Spin Canting and Single-Crystal to Single-Crystal Phase Transformation

Pang-Kuan Chen,[†] Yun-Xia Che,[†] Ji-Min Zheng,*[,†] and Stuart R. Batten[‡]

Department of Chemistry, Nankai University, Tianjin 300071, China, and School of Chemistry, Monash University, Victoria 3800, Australia

Received November 23, 2006. Revised Manuscript Received January 22, 2007

The two-dimensional heteropolynuclear metal-organic framework $[Co_3Zn_2(m\text{-}BDC)_4(\mu_3\text{-}OH)_2(\mu_2\text{-}OH_2)_2(H_2O)_4]\cdot 4.5H_2O$ (**1**) (m-H_2BDC = 1,3-benzenedicarboxylic acid) has been hydrothermally synthesized and characterized by single-crystal X-ray diffraction, infrared spectrum, X-ray powder diffraction, and elemental analysis. Our experimental results signify that the formation of compound **1** is highly medium-selective and temperature-sensitive in the hydrothermal system. Interestingly, **1** undergoes a single-crystal to single-crystal structural phase transition from orthorhombic *Pmna* to monoclinic $P2_1/c$ (**1′**) at very low temperature of about 156.5 K. In this process, we found two topologically different water tapes. More importantly, the magnetic property of the target compound was also intensively investigated in the temperature range of 2−300 K and shows the coexistence of spin canting and field-induced metamagnetism.

Introduction

It is usually recognized that many materials can often experience solid−solid phase transformations as a result of external stimuli (e.g., temperature, pressure, or radiation) and that the structural stability and integrity can be preserved during the transition process. Recently, some successful examples of so-called dynamic structural phase transition (namely, guest exchange based on the selective guest-binding ability of the framework host) have been reported in the literature,[1] and several thermodynamic transformations (mainly triggered by guest removal or solvation/desolvation upon the change of temperature) were also found previously.[2] However, to the best of our knowledge, only one example of solvent rearrangement has been reported[3] in which the crystal undergoes structural transitions between the three temperatures with change of water arrangement.

Porous metal-organic frameworks (MOFs) with unique structural features have attracted considerable interest in the field of supramolecular chemistry and crystal engineering over the past decades, due to their promising applications as catalyst, gas storage, selective separation, sensor, ion exchange, and magnetic materials.[4−6] One of the central objectives in the study of molecular magnetism is the development of robust and reliable structure−property correlations, greatly depending upon the acquisition of a rich variety of magnetic data analyses alongside single-crystal structure characterizations. More recently, the sustained upsurge in the research of the low-dimensional polynuclear paramagnetic transition-metal coordination polymer is driven by the emergence of single-molecule magnets (SMM),[7] single-chain magnets (SCM),[8] and metamagnets[9] in chemistry

* Corresponding author. Tel.: +86-22-23508056. Fax: +86-22-23508056. E-mail: jmzheng@public.tpt.tj.cn.

[†] Nankai University.

[‡] Monash University.

(1) (a) Biradha, K.; Hongo, Y.; Fujita, M. *Angew. Chem., Int. Ed.* **2000**, *39*, 3843. (b) Suh, M. P.; Ko, J. W.; Choi, H. J. *J. Am. Chem. Soc.* **2002**, *124*, 10976. (c) Biradha, K.; Fujita, M. *Angew. Chem., Int. Ed.* **2002**, *41*, 3392. (d) Zeng, M. H.; Feng, X. L.; Chen, X. M. *Dalton Trans.* **2004**, 2217. (e) Choi, H. J.; Suh, M. P. *J. Am. Chem. Soc.* **2004**, *126*, 15844. (f) Dybtsev, D. N.; Chun, H.; Kim, K. *Angew. Chem., Int. Ed.* **2004**, *43*, 5033. (g) Takaoka, K.; Kawano, M.; Tominaga, M.; Fujita, M. *Angew. Chem., Int. Ed.* **2005**, *44*, 2151. (h) Halder, G. J.; Kepert, C. J. *J. Am. Chem. Soc.* **2005**, *127*, 7891. (i) Dobrzańska, L.; Lloyd, G. O.; Esterhuysen, C.; Barbour, L. *Angew. Chem., Int. Ed.* **2006**, *45*, 5856.

(2) (a) Kepert, C. J.; Rosseinsky, M. J. *Chem. Commun.* **1999**, 375. (b) Chen, B.; Eddaoudi, M.; Reineke, T. M.; Kampf, J. W.; O'Keeffe, M.; Yaghi, O. M. *J. Am. Chem. Soc.* **2000**, *122*, 11559. (c) Rather, B.; Zaworotko, M. J. *Chem. Commun.* **2003**, 830. (d) Hanson, K.; Calin, N.; Bugaris, D.; Scancella, M.; Sevov, S. C. *J. Am. Chem. Soc.* **2004**, *126*, 10502. (e) Lee, E. Y.; Suh, M. P. *Angew. Chem., Int. Ed.* **2004**, *43*, 2798. (f) Lee, E. Y.; Jang, S. Y.; Suh, M. P. *J. Am. Chem. Soc.* **2005**, *127*, 6374. (g) Chen, C. L.; Goforth, A. M.; Smith, M. D.; Su, C. Y.; zur Loye, H. C. *Angew. Chem., Int. Ed.* **2005**, *44*, 6673. (h) Nagarathinam, M.; Vittal, J. J. *Angew. Chem., Int. Ed.* **2006**, *45*, 4337. (i) Kondo, M.; Murata, M.; Nishihara, H.; Nishibori, E.; Aoyagi, S.; Yoshida, M.; Kinoshita, Y.; Sakata, M. *Angew. Chem., Int. Ed.* **2006**, *45*, 5461.

(3) Janiak, C.; Scharmann, T. G. *J. Am. Chem. Soc.* **2002**, *124*, 14010.

(4) (a) Noro, S.; Kitagawa, S.; Kondo, M.; Seki, K. *Angew. Chem., Int. Ed.* **2000**, *39*, 2081. (b) Bourne, S. A.; Lu, J. J.; Mondal, A.; Moulton, B.; Zaworotko, M. J. *Angew. Chem., Int. Ed.* **2001**, *40*, 2111. (c) Kitagawa, S.; Kitaura, R.; Noro, S. *Angew. Chem., Int. Ed.* **2004**, *43*, 2334.

(5) (a) Li, H.; Eddaoudi, M.; O'Keeffe, M.; Yaghi, O. M. *Nature* **1999**, *402*, 276. (b) Soo, J.; Whang, D.; Lee, H.; Jun, S. I.; Oh, J.; Jeon, Y. J.; Kim, K. *Nature* **2000**, *404*, 982. (c) Yaghi, O. M.; O'Keeffe, M.; Ockwig, N. W.; Chae, H. K.; Kim, J.; Eddaoudi, M. *Nature* **2003**, *423*, 705.

(6) (a) Chui, S. S. Y.; Lo, S. M. F.; Charmant, J. P. H.; Orpen, A. G.; Williams, I. D. *Science* **1999**, *283*, 1148. (b) Chem, B. L.; Eddaoudi, M.; Hyde, S. T.; O'Keeffe, M.; Yaghi, O. M. *Science* **2001**, *291*, 1021. (c) Halder, G. J.; Kepert, C. J.; Moubaraki, B.; Murray, K. S.; Cashion, J. D. *Science* **2002**, *298*, 1762.

(7) (a) Aronica, C.; Pilet, G.; Chastanet, G.; Wernsdorfer, W.; Jacquot, J. F.; Luneau, D. *Angew. Chem., Int. Ed.* **2006**, *45*, 4659. (b) Ako, A. M.; Hewitt, I. J.; Mereacre, V.; Clérac, R.; Wernsdorfer, W.; Anson, C. E.; Powell, A. K. *Angew. Chem., Int. Ed.* **2006**, *45*, 4926.

(8) (a) Zheng, Y. Z.; Tong, M. L.; Zhang, W. X.; Chen, X. M. *Angew. Chem., Int. Ed.* **2006**, *45*, 6310. (b) Cheng, X. N.; Zhang, W. X.; Zheng, Y. Z.; Chen, X. M. *Chem. Commun.* **2006**, 3603.

(9) (a) Huang, Z. L.; Drillon, M.; Masciocchi, N.; Sironi, A.; Zhao, J. T.; Rabu, P.; Panissod, P. *Chem. Mater.* **2000**, *12*, 2805. (b) Gái, Z. A.; Rutt, O. J.; Smura, C. F.; Overton, T. P.; Barrier, N.; Clarke, S. J.; Hadermann, J. *J. Am. Chem. Soc.* **2006**, *128*, 8530.

10.1021/cm062801s CCC: $37.00
Published on Web 03/29/2007

and materials science. Complicated magnetic anisotropy has a close relationship to metamagnetism. In terms of physical properties, high-nuclearity clusters can retain their magnetization in zero field and at the same time they exhibit quantum tunneling of magnetization (QTM).[10] Metamagnetism as a magnetic phase transition, when compared to the classical ferromagnetism, ferrimagnetism, and antiferromagnetism, still remains largely elusive at this point in time. Thus far, the design and construction of polynuclear complexes and extended networks with predictable magnetic properties is a great challenge to synthesis chemists, even though some empirical rules enable the explanation of magnetic properties and deepen the fundamental understanding of the magnetic origin in a large number of bulk magnetic materials. From another concept of node and spacer, more stable MOFs can be obtained by using metal clusters rather than monometal cores as nodes.[5c,11] Following our interest in the hydrothermal synthesis of novel metamagnet and low-dimensional MOFs (in particular, those containing 3d block cations), herein we wish to report the detailed medium-selective preparation and characterization of a layered heteropolynuclear superstructure $[Co_3Zn_2(m\text{-BDC})_4(\mu_3\text{-OH})_2(\mu_2\text{-OH}_2)_2(H_2O)_4]\cdot 4.5H_2O$, **1**, which undergoes an unusual field-induced metamagnetic phase transition and a single-crystal to single-crystal (SCSC) structural transformation (to **1′**) accompanied by the appearance of disorder within guest water tapes.

Experimental Section

Materials and General Procedures. All chemicals were of reagent grade and were used as received without further purification. The IR spectrum was recorded as KBr pellets on a Nicolet Magna-FT-IR 560 spectrometer in the 4000−400 cm^{-1} region. Elemental analysis for C, H, and N was performed on a Perkin-Elmer 240 analyzer. Inductively coupled plasma (ICP) analysis was carried out on a Perkin-Elmer Optima 3300 DV spectrometer. The thermogravimetric (TG) analysis was investigated on a standard TG-DTA analyzer under nitrogen flow at a heating rate of 2 °C/min for all measurements. The differential scanning calorimetry (DSC) measurements was performed on a NETZSCH DSC 204 with a heating rate of 5 °C/min in the temperature range of −150 to 25 °C. Powder diffraction data were collected with a Rigaku D/max-RC Diffractometer using a Cu target (λ = 1.54060 Å) operated at 50 kV and 180 mA. The instrument was equipped with a diffracted beam graphite monochromator, 1° divergence slit, 0.15 mm receiving slit, and scintillation counter. The data were processed with Rigaku software provided with the diffractometer. The magnetic measurements were performed on the Quantum Design SQUID MPMS XL-7 instruments. The diamagnetism of the sample and sample holder were taken into account.

Synthesis of 1. The mixture of $Zn(NO_3)_2\cdot 6H_2O$ (1.0 mmol), $CoCl_2\cdot 6H_2O$ (1.5 mmol), *m*-H_2BDC (2.0 mmol), and imidazole (1.0 mmol) in the molar ratio of 2:3:4:2 were dissolved in distilled water (8 mL). The pH value was then adjusted to 7 with 2 M KOH. Consequently, the resulting solution was transferred and sealed in a 25 mL Teflon-lined stainless steel vessel, which was heated at 180 °C for 96 h. After the reactor was slowly cooled to room temperature at a rate of 5 °C/h, purple block-shaped crystals were filtered off, washed with distilled water, and dried in air. Yield: 42% based on metal element. ICP analysis of the product gave the contents of Zn and Co as 11.02 and 15.09 wt %, respectively (calcd: Zn, 11.10; Co, 15.01 wt %), indicating a Zn:Co ratio of 2:3. Anal. Calcd (%) for **1**: C, 32.62; H, 3.25. Found: C, 32.65; H, 3.21. IR (KBr): ν (cm^{-1}) = 3607 m, 3323 m, 1610 s, 1558 s, 1370 s, 1368 m, 740 s, 711 m.

Scheme 1. Synthetic Procedure Highlighting the Temperature- and Medium-Selective Formation of the Target Compound

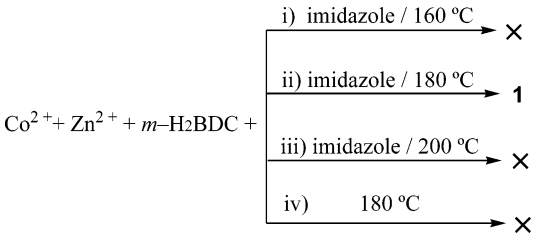

X-ray Crystallographic Determinations. Single-crystal analyses were performed on the Bruker SMART 1000 and RAXIS-RAPID AUTO CCD diffractometer systems (Mo Kα radiation, λ = 0.71073 Å) for **1** and **1′**, respectively. All nonhydrogen atoms were refined anisotropically. Aromatic hydrogen atoms were assigned to calculated positions with isotropic thermal parameters. The hydrogen atoms bonded to the hydroxyl and coordination water oxygen atoms were placed from different maps and refined subject to O−H distance restraints. The free water hydrogen atoms could not be located. CCDC-602476 (**1**) and -611659 (**1′**) contain the supplementary crystallographic data for this paper. These data can be obtained free of charge from The Cambridge Crystallographic Data Centre via www.ccdc.cam.ac.uk/data_request/cif. Crystal data and experimental details are summarized in Table 1 and selected bond lengths and angles are listed in Table 2 (Supporting Information).

Results and Discussion

Crystal Structure Descriptions. The hydrothermal reaction of $Zn(NO_3)_2\cdot 6H_2O$, $CoCl_2\cdot 6H_2O$, *m*-H_2BDC, and imidazole gave rise to purple block-shaped crystals of **1**. Imidazole was not observed in the resulting structures; however, its presence is essential. A series of parallel reactions were carried out (Scheme 1), but failed to give the target compound. Thus, the crystallization and growth of compound **1** was found to be highly selective for the reaction temperature and medium in the hydrothermal synthesis. The function of imidazole is likely as a structure-directing reagent, the precise mechanism of which needs further investigation.

The same single crystal was analyzed by X-ray diffraction at 294 and 150 K. Interestingly, two different space groups were obtained, indicating the occurrence of SCSC structural phase transition. Such a phase transition taking place at about 156.5 K shown in the DSC curve (Figure 1a) was repeatedly observed. Accompanying this switching from *Pmna* (**1**) at 294 K to $P2_1/c$ (**1′**) at 150 K, was an increased level of disorder within the guest water tapes (Scheme 2).

The framework of **1** contains two crystallographically independent octahedral cobalt atoms and one zinc atom (Figure 2a). Valence-sum calculations based on bond lengths

(10) (a) Friedman, J. R.; Sarachik, M. P.; Tejada, J.; Ziolo, R. *Phys. Rev. Lett*. **1996**, *76*, 3830. (b) Thomas, L.; Lionti, F.; Ballou, R.; Gatteschi, D.; Sessoli, R.; Barbara, B. *Nature* **1996**, *383*, 145.
(11) Eddaoudi, M.; Kim, J.; Rose, N.; Vodak, D.; Wachter, J.; O'Keeffe, M.; Yaghi, O. M. *Science* **2002**, *295*, 469.

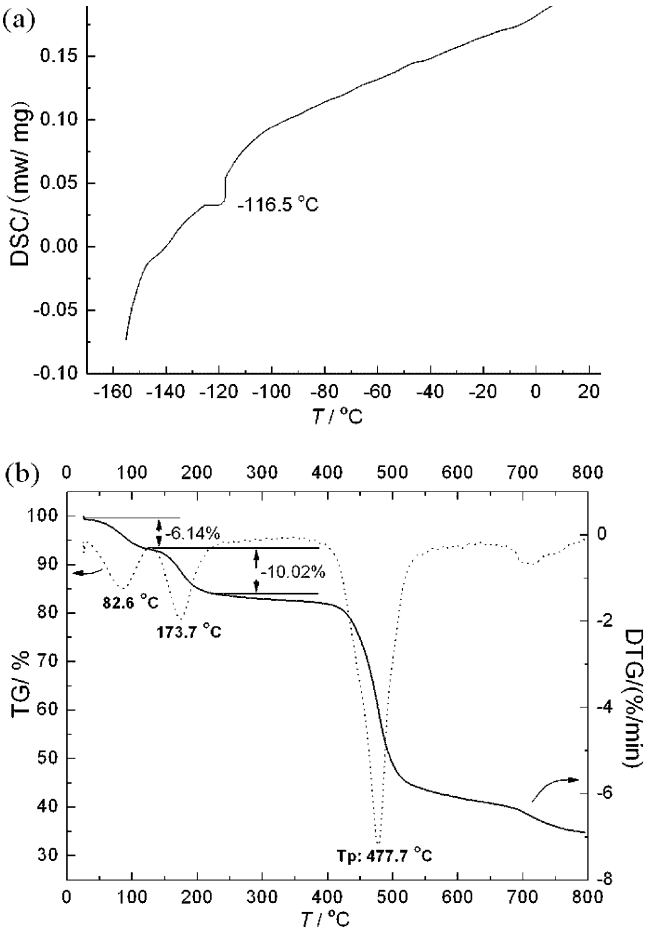

Figure 1. (a) DSC curve at low temperature (−150 to 25 °C) showing the phase transition range, at a heating rate of 5 °C/min; (b) thermogravimetric (TG) curve of the target compound, at a heating rate of 2 °C/min. Solid line: TG; broken line: DTG.

Scheme 2. Schematic Representation of the SCSC Structural Phase Transformation

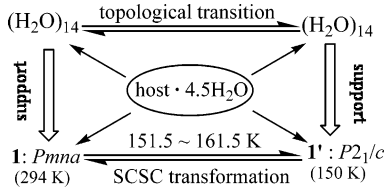

established that all the Co atoms are in the +2 oxidation state,[12] which meets the requirement of charge balance in **1**. Co1 is coordinated by two terminal waters, one μ_2-bridging water, one μ_3-OH group, and two oxygen atoms from different carboxylate groups. Similarly, Co2 is surrounded by two μ_2-OH_2, two μ_3-OH groups, and two $O_{carboxylate}$ atoms. The Zn atoms are tetrahedrally bonded to three $O_{carboxylate}$ atoms and one μ_3-OH.

Heteropentanuclear Co_3Zn_2 clusters are formed in which the central Co2 atom lies on a 2-fold axis, relating one-half of the cluster to the other. On either side of the Co2 atom lie two symmetry-related [$Co1O_6$] octahedra, forming Co trinuclear clusters via an edge-sharing mode. This Co_3 cluster is further connected to two [ZnO_4] tetrahedra in a corner-sharing fashion to generate the heteropentanuclear cluster (Figure 2b). These pentanuclear clusters are then interconnected via bismonodentate, bisbidentate, and monobidentate *m*-BDC ligands to generate a 2D grid with two types of cavities (12.6 × 11.1 and 10.7 × 3.9 Å). The layers parallel to the ac plane can be simplified to a four-connected (4,4) topology when we assign the Co_3Zn_2 cluster as a node and pairs of *m*-BDC ligands as linkers (Figure 2c). The framework remains essentially the same upon lowering the temperature and symmetry in the **1′** phase, although the 2-fold symmetry of the clusters is lost.

A notable feature of the structures, however, are the 1D hydrogen-bonded water tapes formed by the intercalated water molecules (Figure S1a). The tapes contain octameric water clusters consisting of two hexamers inclined to each other, and connected through the sharing of two symmetry-related water positions, which themselves are disordered over two positions (O16/O16′ in **1**; O25/O25′ in **1′**). These clusters are linked to form 1D tapes via interoctamer hydrogen bonding between these disordered waters. Upon lowering the symmetry in **1′**, half of one of the unique water molecules in the tape (O13) become disordered over two positions (to become O29/O29′) (Figure S1b). Importantly, this is the only significant topological difference between the two structural phases. Thermogravimetric (TG) analysis clearly shows two water loss steps below 235 °C (Figure 1b). The first gradual weight loss of 6.14% that takes place between 51 and 120 °C can be attributed to the removal of four lattice waters (calcd: 6.08%). The second weight loss of 10.02% between 120 and 235 °C corresponds to the remaining 6.5 water molecules (calcd: 9.88%). A very strong exothermic peak at 477.7 °C suggests the complete decomposition of the framework. The TG result shows the number of water molecules is consistent with the single-crystal analysis.

Based on PLATON analysis,[13] approximately 17.2% of the crystal volume (4080 $Å^3$) is occupied by lattice water molecules with a volume of 702 $Å^3$ in each unit cell. Crystal structure determinations indicated the monocrystallinity is maintained in the process of transformation, and the macroscopic motif of the host framework in **1′** remains the same as that in **1**. Although the crystal data quality of **1** was poor ($R_1 = 0.1260$), the crucial variation of the cell parameter (γ(**1**) ≡ 90° to β(**1′**) ≡ 92.10(3)°) was quite distinct. Compared with the measured pattern calculated from single-crystal data, the experimental X-ray powder diffraction (XRPD) analysis at room temperature confirmed the structural consistency and phase purity of **1** (Figure 3).

Magnetic Property. Temperature dependence of the magnetic susceptibility χ_m of **1** was measured in a magnetic field of 500 Oe. As shown in Figure 4, the $\chi_m T$ product of each Co_3 unit (7.69 cm^3 K mol^{-1}) at 300 K is larger than that (5.63 cm^3 K mol^{-1}) expected for three magnetically isolated high-spin Co^{II} ions with $S = {}^3/_2$, which have been ubiquitously encountered in those Co-containing complexes reported.[14] This phenomenon should be attributed to the significant orbital contribution of six-coordinate Co^{II}, which is well recognized to be pronounced in octahedral field. The monotonic decrease in $\chi_m T$ until a minimum (3.80 cm^3 K

(12) Brese, N. E.; O'Keeffe, M. *Acta Crystallogr.* **1991**, *B47*, 192.

(13) Spek, A. L. *PLATON, A Multipurpose Crystallographic Tool*; Untrecht University: Utrecht, The Netherlands, 1999.

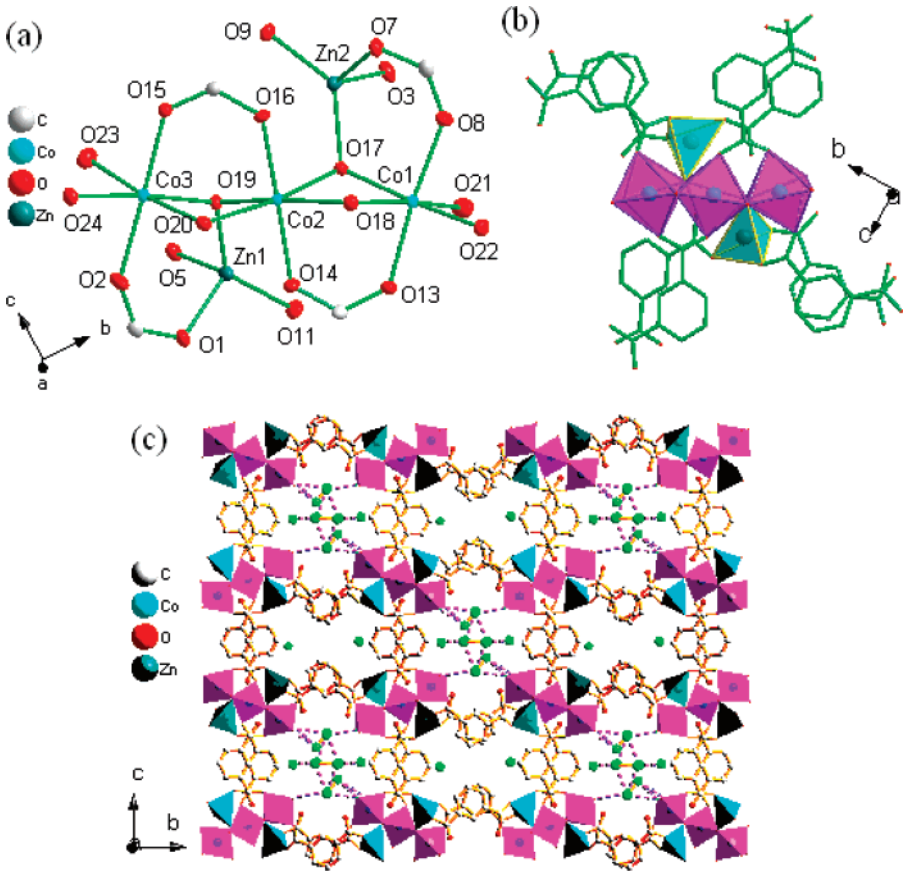

Figure 2. (a) View of the coordination environments of the heterometallic atoms in **1′**. In **1** the two halves of the cluster are related by a 2-fold axis which runs through Co2. (b) The polyhedral presentation of the heteropentanuclear unit as a node connected by *m*-BDC ligand. Zn tetrahedra: blue; Co octahedra: pink. (c) The 2D, four-connected (4,4) topological network in **1′**. Green balls represent the $(H_2O)_{14}$ clusters. Note that the tape-containing channels alternate with other channels which contain only a small number of isolated water molecules.

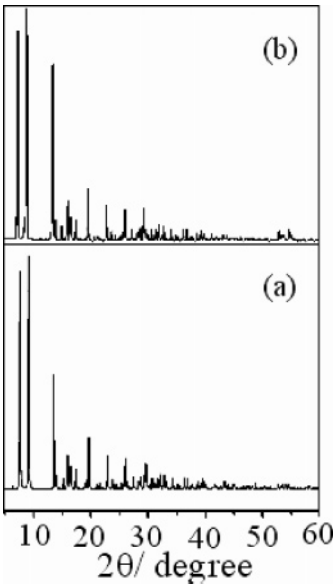

Figure 3. XRPD patterns for compound **1** at room temperature: (a) simulated; (b) experimental.

mol^{-1}) at $T_{min} = 13$ K with cooling temperature is indicative of dominant antiferromagnetic interaction. Upon lowering of the temperature to 5 K, $\chi_m T$ abruptly increases to a maximum (4.07 cm^3 K mol^{-1}). The final rapid drop in $\chi_m T$ below 5 K may arise from the magnetic field saturation effect and/or antiferromagnetic interaction between the layers. These overall tendencies present the typical ferrimagnetic-

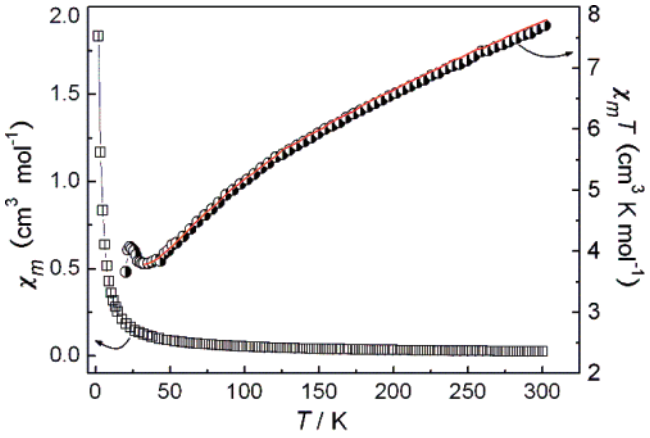

Figure 4. Temperature dependence of the χ_m and $\chi_m T$ product of the target compound. The red solid line shows the best fit from 13 to 300 K.

like behaviors, which are mediated by the mutual competition between ferromagnetic and antiferromagnetic components. Actually, the presence of both ferromagnetic and antiferromagnetic coupling results in a minimum in the $\chi_m T$ vs T measurement. As expected by consideration of the Good-enough−Kanamori rules[15a] and magneto-structural correlation, there exist two main sets of magnetic superexchange

(14) (a) Zeng, M.-H.; Zhang, W.-X.; Sun, X.-Z.; Chen, X.-M. *Angew. Chem., Int. Ed.* **2005**, *44*, 3079. (b) Boudalis, A. K.; Raptopoulou, C. P.; Abarca, B.; Ballesteros, R.; Chadlaoui, M.; Tuchagues, J. P.; Terzis, A. *Angew. Chem., Int. Ed.* **2006**, *45*, 432. (c) Ding, B.-B.; Weng, Y.-Q.; Mao, Z.-W.; Lam, C.-K.; Chen, X.-M.; Ye, B. H. *Inorg. Chem.* **2005**, *44*, 8836.

pathways within the trimeric Co_3 cluster for **1′**: one refers to the μ_3-OH bridge with a large (compared with 90°) Co1−O17−Co2 angle of 96.89(13)°; the other belongs to the carboxyl bridge (Co−OCO−Co) and μ_2-OH_2 water bridge with a smaller angle Co1−O18−Co2 = 87.85(12)°. To achieve noncompensation in spin moments with different spin multiplicities, the coupling interaction through the former bridge must be antiferromagnetic (close to 100°) and that via the latter may be ferromagnetic (smaller than 90°).[15a,16] In addition, dipole−dipole interactions between adjacent layers and exchange effects via interlayer hydrogen bonds are believed to be largely responsible for the antiferromagnetic interaction.[14a]

To estimate the magnetic interactions approximately, the magnetic data above 13 K can be simulated using the HDVV (Heisenberg−Dirac−Van Vleck) spin Hamiltonian for a linear trimeric Co^{II}−Co^{II}−Co^{II} ($S = {}^3/_2$) model[15] under consideration of the orbital angular momentum. The interactions between two terminal Co^{II} centers were omitted. However, the fitting could not reach convergence very well. Thus, a further approximation was employed: χ_{TIP} term was added to take into account the temperature-dependent paramagnetic contribution from the sample. In the meantime, possible paramagnetic impurity ρ of the sample was also taken into account, of which the susceptibility is assumed to follow the Curie law $Ng^2\beta^2S(S+1)\rho/3kT$. By application of the HDVV equation, the following theoretical expression for molar susceptibility may be derived:

$$\chi_m = \chi_{trinuclear}(1-\rho) + \frac{Ng^2\beta^2}{3kT}S(S+1)\rho + 3\frac{A}{B} - \frac{15N\beta^2}{4kT} + \chi_{TIP} \quad (1)$$

$$\chi_{trinuclear} = \frac{Ng^2\beta^2}{4kT}\frac{C}{D} \quad (2)$$

$$A = 3[28u + 9.333 + (22.5u + 4.161)\exp(-3u) + (24.5u - 13.5)\exp(-5u)]$$

$$B = u[7 + 5\exp(-3u) + 3\exp(-5u)]$$

$$C = 165\exp(21X) + 94\exp(12X) + 38\exp(5X) + 10 + 84\exp(18X) + 35\exp(11X) + 10\exp(6X) + \exp(3X) + 35\exp(15X) + 10\exp(10X) + \exp(X)$$

$$D = 5\exp(21X) + 6\exp(12X) + 3\exp(5X) + 2 + 4\exp(18X) + 3\exp(11X) + 2\exp(6X) + \exp(3X) + 3\exp(15X) + 2\exp(10X) + \exp(X)$$

where $u = \lambda/kT$, $\lambda = -177$ cm^{-1}, and $X = J/kT$. The J and g are obtained by minimizing the error $R = \Sigma[(\chi_M T)_{obs} - (\chi_M T)_{calc}]^2/\Sigma[(\chi_M T)_{obs}]^2$. The best-fit parameters from 300 down to 13 K are observed as follows: $J = -5.53$ cm^{-1}, $g = 2.29$, $\rho = 0.012$, and $\chi_{TIP} = 260 \times 10^{-6}$ cm^3 mol^{-1} with $R = 3.58 \times 10^{-4}$. The negative J value demonstrates that Co^{II} spins bridged through pure oxygen bridging are antiferromagnetically coupled above 13 K.

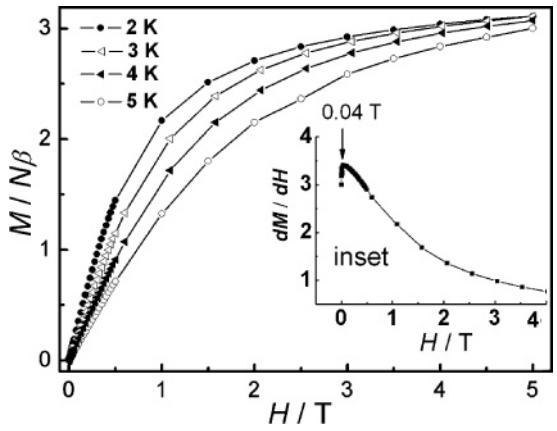

Figure 5. Field-dependent magnetization of **1′** at different temperatures. The inset shows the $\delta M/\delta H$ curve at 2 K.

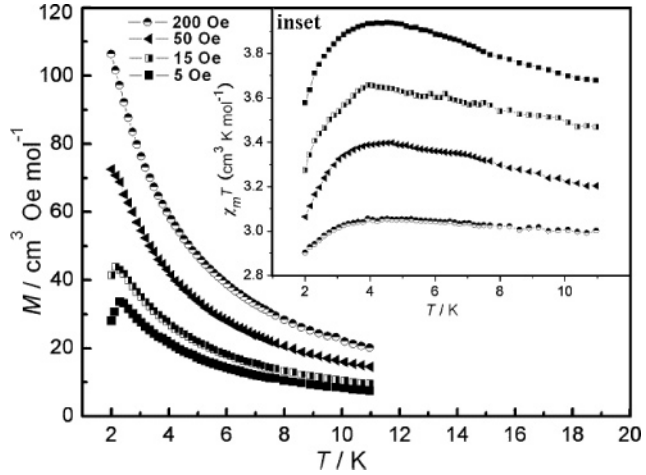

Figure 6. Temperature-dependent field-cooled magnetization (FCM) of **1′**. Inset: graph of $\chi_M T$ vs T for **1′** at different applied fields.

The magnetic behaviors of complex **1′** are further characterized by temperature- and field-dependent magnetization measurements in the low-temperature region. As illustrated in Figure 5, the isotherm magnetizations clearly display a drastic rise in M vs H at the beginning of the field, and then smoothly increased to the saturation magnetization (M_s) of about 3.11 $N\beta$ per Co_3 unit at 5 T. The experimentally observed magnetization is far from the value of 9.0 $N\beta$ anticipated for three independent Co^{II} with $S = {}^3/_2$ ground state. The field-cooled (FC) magnetizations under different applied fields were given in Figure 6. At low field of 5 and 15 Oe, the FC curve shows a maximum at ca. 2.2 K, which disappears at higher field of 50 and 200 Oe. This indicates an antiferromagnetic ordering of ferrimagnetic layers, and that the external field is large enough to overcome the intralayer antiferromagnetic interactions to result in an ordered ferromagnetic phase below 2.2 K. These features are characteristic of metamagnetic behaviors, which are confirmed by the field dependence of magnetization (inset of Figure 7). The sigmoidal shape of the $M/N\beta$ vs H curve at 2 K suggests the field-induced transition from an antifer-

(15) (a) Kahn, O. *Molecular Magnetism*; Wiley-VCH: New York, 1993. (b) Higgs, T. C.; Spartalian, K.; O'Connor, C. J.; Matzanke, B. F.; Carrano, C. J. *Inorg. Chem.* **1998**, *37*, 2263.
(16) Zeng, M .H.; Gao, S.; Chen, X. M. *Inorg. Chem. Commun.* **2004**, *7*, 864.

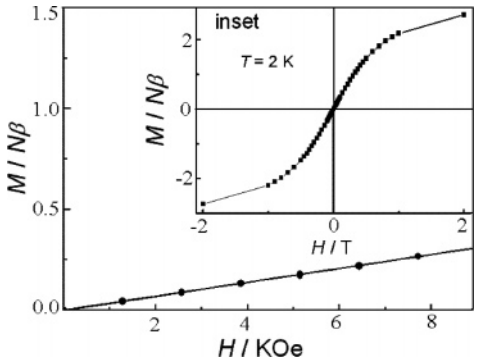

Figure 7. Field dependence of magnetization of **1′** in the low-field region at 2 K. Inset: the hysteresis loop at 2 K.

romagnetic to a ferromagnetic state.[17] The critical field *Hc* = 400 Oe for such a metamagnetic transition is approximately determined by the sharp peak of $\delta M/\delta H$ (inset of Figure 5). The presence of weak ferromagnetism (also called "canted antiferromagnetism") and the small magnetization at high field might be explained by possible spin canting, resulting from the single-ion magnetic anisotropy and/or the lack of inversion center between the neighboring Co ions.[18] For a weak ferromagnet due to spin canting, the magnetic behavior should be quite field-dependent. As expected, the $\chi_m T$ vs T shows the maximum at low temperatures *decreases* with *increasing* applied field (inset of Figure 6). From another viewpoint, the spin-canted ferromagnetism can be evidenced by the fact that the resulting magnetizations ($M-H$ plots) increase rapidly at very low fields, whereas the magnetizations increase slowly and linearly in high-field region. Extrapolating the reversible linear part of the sigmoidal shape curve to zero field gives a magnetization value of 0.314 $N\beta$ (Figure 7). Assuming this to be the uncompensated magnetization, the spin-canting angle is estimated to be about 2.0°.[19] Further analysis reveals compound **1′** is a soft ferromagnet without detectable coercivity and magnetic hysteresis. To be noted, the effect of structural phase transition on the magnetic property of **1** was not evident, which can be explained by the fact that the magnetic exchange situations between Co^{II} ions in **1** and **1′** remain the same, as well as a little change in bond parameters.

Conclusions

In conclusion, a novel heteropolynuclear spin-canting metamagnet has been successfully obtained and well magnetically characterized from the magneto-structural point of view. This paper not only highlights an unusual metamagnetic phase transition and SCSC structural phase transition but also presents two topologically different 1D water tapes between the two phases. It is of considerable importance to study the guest behavior in achieving better insight into the interesting single-crystal interconversion. We believe this work will greatly improve our knowledge about the cooperative effect between guest molecule and crystal host, as well as the unique structural characteristics of water clusters. Furthermore, the foregoing crystallization selectivity enhances our scientific understanding of crystal growth conditions. Attempts in progress to incorporate other guest molecules during the design process will be useful.

Acknowledgment. This work was supported by the National Natural Science Foundation of China (50572040).

Supporting Information Available: X-ray crystallographic files in CIF format, tables of crystal data, bond lengths and angles, hydrogen bond parameters, and structure graphics. This material is available free of charge via the Internet at http://pubs.acs.org.

CM062801S

(17) (a) Tao, J.; Zhang, Y.-Z.; Bai, Y.-L.; Sato, O. *Inorg. Chem*. **2006**, *45*, 4877. (b) Das, A.; Rosair, G. M.; EI Fallah, M. S.; Ribas, J.; Mitra, S. *Inorg. Chem*. **2006**, *45*, 3301.

(18) (a) Gao, E.-Q.; Wang, Z.-M.; Yan, C.-H. *Chem. Commun*. **2003**, 1748. (b) Rodríguez, A.; Kivekäs, R.; Colacio, E. *Chem. Commun*. **2005**, 5228.

(19) Bellitto, C.; Federici, F.; Colapietro, M.; Portalone, G.; Caschera, D. *Inorg. Chem.* **2002**, *41*, 709.